Catalysis Science & Technology

ROYAL SOCIETY OF CHEMISTRY

COMMUNICATION

View Article Online
View Journal | View Issue

Cite this: *Catal. Sci. Technol.*, 2022, **12**, 5252

Received 4th July 2022,
Accepted 5th August 2022

DOI: 10.1039/d2cy01185a

rsc.li/catalysis

Deciphering the reaction mechanisms of photothermal hydrogen production using H/D kinetic isotope effect†

Sara El Hakim, Tony Chave and Sergey I. Nikitenko *

H/D kinetic isotope effect has been employed to study the mechanism of the thermally assisted photocatalytic hydrogen production over noble metal-free Ti@TiO_2 core–shell nanoparticles. We have found that the observed large H/D isotope separation factor (α_H = 11.3 ± 1.7–6.2 ± 0.9) is due to the electron hole-mediated cleavage of OH bond. It was concluded that strong H/D isotopic selectivity is associated with significant photothermal effect.

Production of "green" hydrogen is of paramount importance for clean and secure energy systems. Up to date, the baseline technology to access "green" H_2 is the water-electrolysis, where the main challenges are the elevated cost and the use of critical raw materials.[1] Photocatalysis is potentially a very promising way to split water and produce H_2 directly from solar light without the use of electricity. However, achieving such a process with high efficiency continues to be a challenge. Introducing heat into photocatalytic processes has attracted much attention in the last decade because it may significantly improve the photoconversion efficiency.[2,3] However, literature survey revealed a lack of consensus about the origin of temperature effect in photocatalytic processes. At present, there are three hypotheses explaining the photothermal effect in solutions:

(i) temperature dependent competition between water molecules and sacrificial reagents at the catalyst surface,[4]

(ii) temperature effect on the migration of intermediates in the vicinity of active sites of catalysts,[5] and

(iii) positive temperature effect on charge carrier mobility and interfacial charge transfer.[6]

The H/D kinetic isotope effect (KIE) can provide insightful information about the dominating reaction pathway of photocatalytic H_2 formation. In the gas phase, H/D KIE revealed a critical role of the photoexcited hot carriers in the photocatalytic steam reforming of CH_4/CD_4 mixture over Rh/TiO_2 catalyst.[7] In aqueous solutions, the KIE is usually studied by comparing the photocatalytic reaction rates in H_2O and D_2O.[8–10] Observed at such conditions KIE represents the overlap of primary isotope effect referred to the cleavage of chemical bonds and solvent isotope effect. Moreover, the H/D isotopic exchange between the solvent and reacting species can mask the actual source of hydrogen in photocatalytic process. The physico-chemical properties of D_2O, such as polarity, viscosity, dielectric constant *etc.*, are different from those of H_2O and tend to be dependent on temperature.[11] Therefore, comparison of the hydrogen formation rate in neat H_2O and D_2O is hardly applicable for understanding the origin of thermally assisted photocatalytic process. Recently, photocatalytic hydrogen production was studied in H_2O/D_2O mixtures over platinized TiO_2 in the presence of formaldehyde.[12] It was shown that the reaction rate decreases with increasing D_2O concentration. However, neither the effect of temperature nor the H/D isotopic selectivity were investigated. Herein, we report for the first time the effect of temperature on H/D isotopic selectivity during the photocatalytic hydrogen production using H_2O/D_2O mixtures over noble metal-free Ti@TiO_2 core–shell photocatalyst in the presence of 1 M glycerol (Glyc) as sacrificial reagent.

The Ti@TiO_2 photocatalyst has been prepared by sonohydrothermal treatment of metallic titanium nanoparticles (NPs) in pure water at 200 °C under the assistance of 20 kHz ultrasound as described previously.[13–15] The particles are composed of quasi-spherical 50–150 nm Ti^0 core coated by 10–20 nm of TiO_2 anatase nanocrystals. Additional data about the catalyst preparation and their morphology are presented in the ESI† (Fig. S1–S3). The absorption spectrum of Ti@TiO_2 nanoparticles is composed of interband and intraband transitions of metallic Ti spanning from UV to NIR spectral range and a TiO_2 bandgap localized at 220–350 nm.[14,15]

ICSM, CEA, CNRS, ENSCM, Univ Montpellier, Marcoule, France.
E-mail: serguei.nikitenko@cea.fr

† Electronic supplementary information (ESI) available: Experimental details and additional figures. See DOI: https://doi.org/10.1039/d2cy01185a

The photocatalytic experiments were performed in a thermostated argon-flow cell adapted to the outlet gas analysis by mass spectrometer. Irradiation was carried out using the white light of ASB-XE-175 W xenon lamp equipped with ozone blocking coating. The light power measured by X1-1 Optometer was found to be equal to 8.9 W and 0.6 W for vis/NIR (400–1100 nm) and UV (300–420 nm) spectral ranges respectively. The temperature inside the photoreactor was controlled using Julabo F12 thermostat. More details can be found in the ESI† (Fig. S4). Obtained results were analysed according to three parameters: (i) the total hydrogen formation rate, $R(\sum H_2)$, calculated as the sum of the rates of three released hydrogen isotopic species $R(\sum H_2) = R(H_2) + R(HD) + R(D_2)$, (ii) the apparent activation energy, E_a, for total hydrogen production, and (iii) the isotopic selectivity measured as H/D isotope separation factor, $\alpha_H = (H/D)/(H/D)_0$, where the initial ratio $(H/D)_0$ was equal to the molar composition of H_2O/D_2O mixture with 1 M Glyc, and the experimental (H/D) ratio was measured in released hydrogen for H_2, HD and D_2 isotopologues using mass spectrometry as it described in the ESI.†

Fig. 1 depicts the emission profiles of H_2, HD, and D_2 species during photolysis of 50 mol% H_2O/50 mol% D_2O mixture under stepwise heating. Obtained results point out a strong effect of temperature on the kinetics of hydrogen production and a significant enrichment of the formed hydrogen gas with light isotope. It is noteworthy that the formation of hydrogen is not observed when the Xe lamp is off even at 94 °C highlighting the photonic origin of hydrogen formation in studied system. Fig. 2 demonstrates a strong increase of photocatalytic hydrogen production with increasing of bulk temperature whatever the H_2O/D_2O ratio. In addition, it can be seen that $R(\sum H_2)$ gradually decreases with the increase of D_2O content.

In the whole range of studied H_2O/D_2O ratios, mass spectrometric measurements indicate the absence of CO_2 or other carbon-containing gases during the photothermal process in agreement with our previous results in H_2O solutions.[15] On the other hand, photolysis leads to acidification of the reaction mixture. HPLC analysis reveals the presence of glyceraldehyde and glyceric acid in photolytes (ESI† Fig. S5) indicating the oxidation of C–OH group of glycerol without decarboxylation.

The calculated apparent activation energy E_a depends on D_2O concentration such that E_a is equal to 23 ± 3 kJ mol^{-1} for $[D_2O] < 50$ mol% and 39 ± 5 kJ mol^{-1} for $[D_2O] \geq 50$ mol% (Fig. 3). Nevertheless, both E_a values are much lower than the typical dissociation energy of chemical bonds indicating that the cleavage of chemical bond is not involved in the rate-determine stage. The influence of H_2O/D_2O ratio on $R(\sum H_2)$ and E_a values could be understood in terms of solvent isotope effect. In H_2O/D_2O mixtures at $[D_2O] \geq 50$ mol%, water mainly presents as HDO and D_2O molecules because of fast equilibrium:[16]

$$H_2O + D_2O \leftrightarrows 2HDO,\ K_{eq} = 3.4\ (T = 300\ K) \quad (1)$$

The increase of hydrogen bonds energy of water on *ca.* 5% upon deuteration results in the modification of hydrogen-bonded supramolecular network.[17,18] Consequently, the

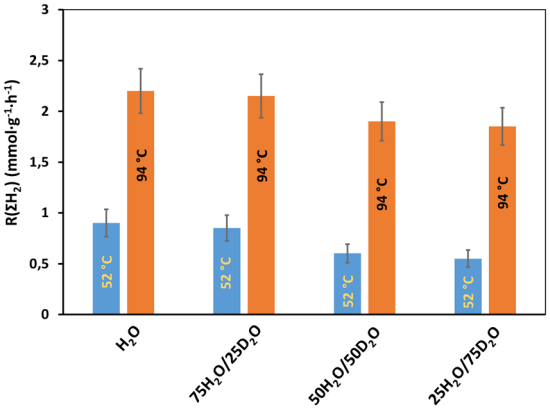

Fig. 2 Total hydrogen formation rate at different H_2O/D_2O ratios obtained at 52 and 94 °C. At other studied temperatures, a similar trend was observed.

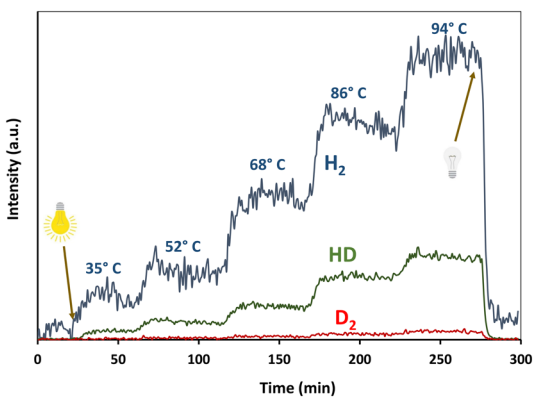

Fig. 1 Emission profiles of H_2, HD, and D_2 species during photolysis of 50 mol% H_2O/50 mol% D_2O mixture in the presence of Ti@TiO_2 NPs and 1 M glycerol irradiated with Xe-lamp under Ar-flow.

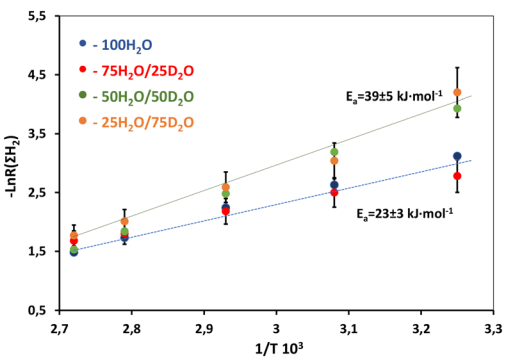

Fig. 3 Arrhenius plots for photothermal hydrogen production at different H_2O/D_2O ratios.

diffusion of intermediate species formed after photoexcitation would require a higher activation barrier in solutions enriched with D_2O compared to H_2O. However, the $R(\sum H_2)$ and E_a values are unable to provide more insightful information about the mechanism of photothermal effect in studied system.

On the other hand, the studied photocatalytic process exhibits a high H/D isotopic selectivity. As demonstrated in Fig. 4a, the isotope separation factor, α_H, varies from 11.3 ± 1.7 to 6.2 ± 0.9 depending on temperature and H_2O/D_2O ratio. Such significant α_H values cannot be attributed to the relatively small solvent isotope effect or to the KIE during diffusion of intermediates. In contrast to $R(\sum H_2)$, the α_H values decrease with temperature and follow a zero-point energy approximation, expressed as $\alpha_H = \exp(\Delta E/RT)$ shown in Fig. 4b, where ΔE = 5.89 kJ mol^{-1} is the zero-point energy difference between OH and OD bonds.[19] It should be noted that the apparent value of ΔE_{app} = 6.25 ± 0.64 kJ mol^{-1} calculated from the experimental data for $75H_2O/25D_2O$ mixture is fairly close to the theoretical ΔE value. However, for the mixtures with $[D_2O] \geq 50$ mol% the calculated ΔE_{app} = 2.13 ± 0.25 kJ mol^{-1} is lower than the theoretical one. Strictly speaking, the ΔE_{app} obtained from the kinetic experiments does not represent the difference of vibrational energies for OH and OD species retain at the absolute zero of temperature, but rather some effective energy value depending on the reaction medium also. In terms of Eyring transition state theory, the isotope separation factor is expressed as a difference of the free energies of activation, $\Delta G^{\neq}$, for the transition states involving H- and D-isotopologues as following:[20]

$$\alpha_H = \exp\{(\Delta G_D^{\neq} - \Delta G_H^{\neq})/RT\} \quad (2)$$

$$\Delta G^{\neq} = \Delta H^{\neq} - T\Delta S^{\neq} \quad (3)$$

Therefore, ΔE_{app} can be approximated as $\Delta E_{app} \approx \Delta G_D^{\neq} - \Delta G_H^{\neq}$. In general, the enthalpy of activation, $\Delta H^{\neq}$, is dominated by the difference in the vibrational energies of the transition state and the reactant state. On the other hand, the entropy of activation, $\Delta S^{\neq}$, is sensitive to the reorganization of solvent network during product formation. As mentioned above, D_2O is a more structured solvent than H_2O. Hence, the relative activation entropy modification during the transition state formation would be somewhat larger in D_2O than in H_2O leading to the decrease of ΔE_{app} value as it is observed in the experiments.

Surprisingly, our study reveals an $E_a - \alpha_H$ paradox. While the E_a values indicate that the cleavage of chemical bonds is not involved in the limiting stage, the isotopic selectivity values point to the contrary. This paradox can be overcome taking into account that in the systems with TiO_2-based catalysts the cleavage of O–H bond is mediated by a charge transfer to the photogenerated electron hole, h^+, which sharply reduces the required activated energy.[8,10,21] Consequently, we can infer that the observed H/D KIE is attributed to the difference in the rate constants of h^+-mediated dissociation of O–H and O–D bonds. It is also conceivable that the observed photothermal effect deals with the dynamics of h^+ production. Recent spectroscopic investigations of photocatalysis over TiO_2 NPs by time-resolved laser flash photolysis revealed a thermally activated equilibrium of shallowly trapped holes with free holes exhibiting a high oxidation potential.[22] According to this study, the increase of temperature leads to an increase in the concentration of the highly reactive free holes at the surface of catalyst. The E_a of h^+ polaron hopping in anatase calculated using DFT is equal to *ca.* 29 kJ mol^{-1},[23] which is quite close to the E_a values found in this work. In addition, photoelectrochemical study of Park *et al.*[6] pointed out a positive relationship between the reaction temperature and h^+ mobility in Pt/TiO_2 photocatalyst. These results strongly support the contribution of h^+ mobility into the overall photothermal effect.

It is important to note that the photothermal H_2 production over $Ti@TiO_2$ NPs is more efficient in aqueous glycerol solutions than in pure water indicating that the splitting of OH groups from glycerol contributes stronger to hydrogen formation than those of water.[15] Rapid isotopic exchange of hydrogen between hydroxyl-groups of glycerol, R-OH, and water provides the H/D isotopic ratio in OH groups of glycerol very close to those in H_2O/D_2O mixture:

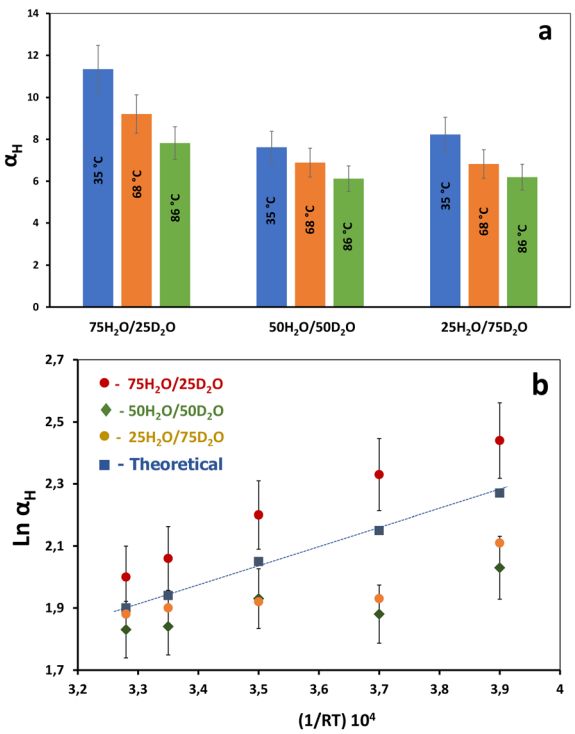

Fig. 4 a) Evolution of H/D isotope separation coefficient with temperature and H_2O/D_2O ratio. b) Temperature dependence of H/D isotope separation coefficient in terms of OH/OD zero-point energy approximation for different H_2O/D_2O ratios. Dotted line indicates theoretical plot calculated for ΔE = 5.89 kJ mol^{-1}.

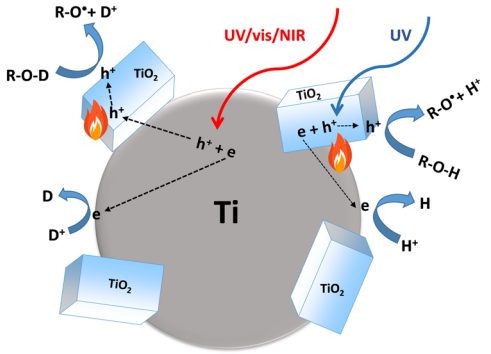

Scheme 1 Schematic representation of the photothermal hydrogen production in H_2O/D_2O mixtures over $Ti@TiO_2$ catalyst in the presence of glycerol.

$$\text{R-OH} + D_2O \leftrightarrows \text{R-OD} + \text{HDO} \quad ([D_2O] > [H_2O] \gg [\text{Glyc}]) \qquad (4)$$

When we account for harmonic approximation, we can estimate that the difference of vibrational energies for OH and OD groups is the same for glycerol and water. In such case, the H/D isotopic selectivity would be practically the same for OH/OD bonds cleavage for water and glycerol molecules:

$$\alpha_H = \frac{k_{R\text{-}OH}}{k_{R\text{-}OD}} \qquad (5)$$

The principal steps of the process leading to the photothermal hydrogen production and hydrogen isotope fractionation are illustrated in the Scheme 1. It is noteworthy that the Ti^0 metallic core in $Ti@TiO_2$ NPs acts as an electron sink providing an electron–hole separation in a similar way as in TiO_2 loaded with noble metal NPs.[14] The quantum tunneling of e^- and H^+ species are not included in the photothermal mechanism since these processes are known to be weakly dependent on bulk temperature.[24]

In conclusion, the H/D isotopic fractionation measured in H_2O/D_2O mixtures provides more insightful information about the mechanism of thermally assisted photocatalytic hydrogen formation compared to the global hydrogen formation rate or apparent activation energy. In the system with $Ti@TiO_2$ photocatalyst, large H/D isotope separation coefficient and its variation with bulk temperature clearly pointed out a strong involvement of the hole-mediated O–H bond cleavage in the limiting stage of the process. On the other hand, less significant influence of solvent on the efficiency of photothermal hydrogen production also cannot be completely ignored. It would appear that strong H/D KIE expressed as isotopic selectivity is associated with a significant photothermal effect and *vice versa*. Indeed, Hisatomi *et al.* reported a relatively small photothermal effect in the process of hydrogen production over $(Ga_{1-x}Zn_x)(N_{1-x}O_x)/Rh_{2-y}Cr_yO_3$ photocatalyst in the presence of different sacrificial reagents (E_a = 7–8 kJ mol^{-1}).[25] The authors concluded that mass diffusion is a limiting stage of hydrogen production with studied photocatalyst. This conclusion is consistent with the results of our work pointed out the importance of chemical bond cleavage at the active site of photocatalyst to observe strong photothermal effect.

Conflicts of interest

There are no conflicts to declare.

Acknowledgements

The authors gratefully acknowledge Dr. Sabine Valange and Dr. Prince Amaniampong (IC2MP, Poitiers) for providing HPLC analysis.

References

1 *Hydrogen production by electrolysis*, ed. A. Godula-Jopek and D. Stolten, Wiley-VCH, Weinheim, Germany, 2015.
2 D. Mateo, J. L. Cerrillo, S. Durini and J. Gascon, *Chem. Soc. Rev.*, 2021, **50**, 2173–2210.
3 S. Luo, X. Ren, H. Lin, H. Song and J. Ye, *Chem. Sci.*, 2021, **12**, 5701–5719.
4 F. Parrino, P. Conte, C. De Pasquale, V. A. Laudicina, V. Loddo and L. Palmisano, *J. Phys. Chem. C*, 2017, **121**, 2258–2267.
5 Y. Nishijima, K. Ueno, Y. Kotake, K. Murakoshi, H. Inoue and H. J. Misawa, *J. Phys. Chem. Lett.*, 2012, **3**, 1248–1252.
6 G. Kim, H. J. Choi, H. Kim, J. Kim, D. Monllor-Satoca, M. Kim and H. Park, *Photochem. Photobiol. Sci.*, 2016, **15**, 1247–1253.
7 H. Song, X. Meng, Z.-J. Wang, Z. Wang, H. Chen, Y. Weng, F. Ichihara, M. Oshikiri, T. Kako and J. Ye, *ACS Catal.*, 2018, **8**, 7556–7565.
8 P. K. J. Robertson, D. W. Bahnemann, L. A. Lawton and E. Bellu, *Appl. Catal., B*, 2011, **108-109**, 1–5.
9 T. Hisatomi, K. Takanabe and K. Domen, *Catal. Lett.*, 2015, **145**, 95–108.
10 S. Yu and P. K. Jain, *Angew. Chem., Int. Ed.*, 2020, **59**, 22480–22483.
11 D. M. Quinn, Theory and practice of solvent isotope effects, in *Isotope effects in chemistry and biology*, ed. A. Kohen and H.-H. Limbach, CRC Press, Boca Raton, USA, 2006.
12 H. Belhadj, S. Hamid, P. K. J. Robertson and D. W. Bahnemann, *ACS Catal.*, 2017, **7**, 4753–4758.
13 S. I. Nikitenko, T. Chave, C. Cau, H.-P. Brau and V. Flaud, *ACS Catal.*, 2015, **5**, 4790–4795.
14 S. I. Nikitenko, T. Chave and X. Le Goff, *Part. Part. Syst. Charact.*, 2018, **35**, 1800265.
15 S. El Hakim, T. Chave, A. A. Nada, S. Roualdes and S. I. Nikitenko, *Front. Catal.*, 2021, **1**, 669260.
16 M. Kakiuchi, *Geochim. Cosmochim. Acta*, 2000, **64**, 1485–1492.
17 S. Scheiner and M. Cuma, *J. Am. Chem. Soc.*, 1996, **118**, 1511–1521.
18 C. Shi, X. Zhang, C.-H. Yu, Y.-F. Yao and W. Zhang, *Nat. Commun.*, 2018, **9**, 481.
19 W. A. Van Hook, *Nukleonika*, 2011, **56**, 217–240.

20 K. J. Laidler and M. C. King, *J. Phys. Chem.*, 1983, **87**, 2657–2664.
21 T. A. Kandiel, I. Ivanova and D. W. Bahnemann, *Energy Environ. Sci.*, 2014, **7**, 1420–1425.
22 D. W. Bahnemann, M. Hilgendorff and R. Memming, *J. Phys. Chem. B*, 1997, **101**, 4265–4275.
23 J. J. Carey, J. A. Quirk and K. P. McKenna, *J. Phys. Chem. C*, 2021, **125**, 12441–12450.
24 P. R. Schreiner, *J. Am. Chem. Soc.*, 2017, **139**, 15276–15283.
25 T. Hisatomi, K. Maeda, K. Takanabe, J. Kubota and K. Domen, *J. Phys. Chem. C*, 2009, **113**, 21458–21466.

